

Effect of Adjacent Layers on Crystallization and Magnetoresistance in CoFeB/MgO/CoFeB Magnetic Tunnel Junction

Chando Park¹, Yung-Hung Wang², David E. Laughlin¹, and Jian-Gang Zhu¹

¹Data Storage Systems Center, Carnegie Mellon University, Pittsburgh, PA 15213 USA

²Electronics Research and Service Organization, Industrial Technology Research Institute, Division of Nanoelectronic Device Technology, Hsinchu, Taiwan 310, R.O.C.

Crystallization must occur in order to obtain lattice matching between CoFeB and MgO in amorphous CoFeB/MgO/amorphous CoFeB magnetic tunnel junction (MTJ). However, the interface layer effect on the crystallization behavior is not yet clear. An aim of our experiments was to investigate the effects of various layers including Ta, MgO, Ru, and NiFe on the crystallization and transport properties in CoFeB/MgO/CoFeB MTJs deposited on SiO₂/Si and glass. It was found that the onset of crystallization of CoFeB and its specific orientation were dependent on the layer adjacent to CoFeB. The effects of crystallization on transport properties are also discussed.

Index Terms—CoFeB, crystallization, MgO barrier.

I. INTRODUCTION

MgO based magnetic tunnel junctions (MTJs) show a high magnetoresistance (MR) effect and are currently the most promising ones for the application in magnetoresistive devices such as magnetic random access memory (MRAM), magnetic read heads and magnetic sensors [1], [2]. For MTJs with crystalline MgO barrier, the tunneling probabilities of the electrons depend on the symmetries of the Bloch states at the Fermi level and symmetry dependent decay of the evanescent states in the MgO barrier [3], [4]. That is, only electrons having an s angular momentum character can easily tunnel through the MgO tunnel barrier, while electrons without s angular momentum are difficult to tunnel through. In particular, in the [100] direction of crystalline CoFe/crystalline MgO/crystalline CoFe structure, only those majority spin electrons that contribute to tunneling have s angular momentum; minority spin electrons, in contrast, do not have s angular momentum, therefore resulting in high MR [4]. Thus, to obtain high MR in amorphous CoFeB/crystalline MgO/amorphous CoFeB MTJs, an annealing step is necessary in order to produce crystallized bcc CoFeB (100)/MgO (100)/crystallized bcc CoFeB (100) [5].

It is well known that crystallization behavior can be affected by the interface [6]. Since the MTJ structure consists of several layers, the layers adjacent to the CoFeB layer can affect the orientation of the CoFeB layer during crystallization. However, the annealing effects of adjacent layers of CoFeB on the microstructure of these MTJs have not been clarified. In this paper, we present the experimental results of our investigation of the annealing effects of those layers adjacent to the CoFeB layer on the structural and transport properties of sputtered CoFeB/MgO/CoFeB magnetic tunnel junctions. Since the crystallization of the amorphous CoFeB layer can occur from

both the interfaces of the CoFeB layer, we focused on these two interfaces.

II. EXPERIMENTAL PROCEDURES

Layered stacks of MgO/CoFeB/MgO, Ta 10/PtMn 30/CoFe 1.5/Co₆₀Fe₂₀B₂₀ 3/MgO 2/Co₆₀Fe₂₀B₂₀ 5/Ta 5 (in nm) (Sample A), Ta 10/PtMn 30/CoFe 3/Ru 0.8/Co₆₀Fe₂₀B₂₀ 3/MgO 2/Co₆₀Fe₂₀B₂₀ 5/Ru 5 (in nm) (Sample B), and Ta 20/Co₆₀Fe₂₀B₂₀ 5/MgO 2/Co₆₀Fe₂₀B₂₀ 5/NiFe 3/IrMn 25/Ta 5 (in nm) (Sample C) were deposited on glass and oxidized silicon substrates using an RF/DC sputtering system. The tunnel barrier layer was formed by RF sputtering from MgO target. All of the junctions were patterned by photolithography and ion beam etching. The junction size was $6 \times 2 \mu\text{m}^2$. All the samples were annealed using rapid thermal annealing (RTA). The identity of the phase in the films was determined by conventional $\theta - 2\theta$ x-ray diffraction (XRD) and in-plane XRD. The interface of the films was investigated by high resolution transmission electron microscopy (HRTEM), and the magnetic properties were measured at room temperature using a vibrating sample magnetometer (VSM). The magnetoresistance (MR) transfer curve was measured using a four-point probe measurement system.

III. RESULTS AND DISCUSSION

To investigate whether an MgO barrier would induce the orientation (100) in CoFeB during annealing—the required orientation in CoFeB/MgO/CoFeB MTJs for high MR—bilayers of MgO/CoFeB were deposited on glass substrates and annealed at 380°C and 400°C for 30 min. To increase the signal for the XRD measurement, the stack included 7 bilayers of MgO/CoFeB. The XRD patterns for the stacks of [MgO 1.2–2 nm/CoFeB 4 nm]₇ are shown in Fig. 1. The 2 nm MgO multilayer clearly induced a (100) bcc texture in CoFeB during annealing at 380°C for 30 min, indicating the epitaxial relationship between MgO and CoFeB. When MgO thickness was reduced from 2 to 1.2 nm,

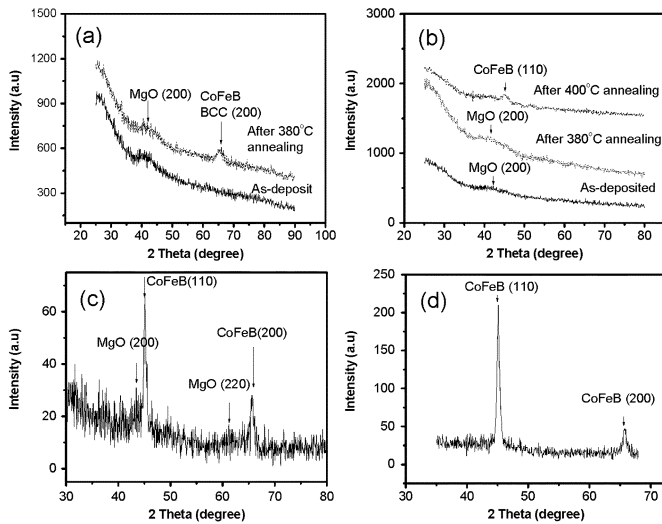


Fig. 1. Conventional θ - 2θ XRD patterns for as deposited and annealed (a) [MgO 2/CoFeB 4]₇ and (b) [MgO 1.2/CoFeB 4]₇ films in nm. In-plane XRD patterns at a 2° grazing incident angle for as deposited and annealed (c) [MgO 2/CoFeB 4]₇ and (d) [MgO 1.2/CoFeB 4]₇ films in nm.

there were no peaks in the XRD pattern after annealing at 380°C for 30 min, indicating the amount of crystallization is negligible in the CoFeB layers. A (110) peak appeared only after annealing at 400°C for 30 min, suggesting that the 1.2 nm MgO layer, which as seen in Fig. 1(b) has a poor texture, did not induce a strong (100) texture in CoFeB layers. Since either face centered cubic or body centered cubic structure can exist in the composition of Co₆₀Fe₂₀B₂₀ depending on the preparation condition [7], in-plane XRD measurements were used to identify the crystallized phase of CoFeB. Note that the peak around 65° only appears for the bcc (200) plane. From Fig. 1(c) and (d), the structure of the crystallized CoFeB is bcc. In bcc structure, {110} planes, which have the lowest energy, can easily develop during annealing. With a strong (100) textured MgO layer, which can be seen in Fig. 1(a) and (c), (200) orientation in CoFeB was also induced. However, with a weak (100) textured MgO layer (1.2 nm) in Fig. 1(b) and (d), (110) orientation in CoFeB was mostly induced and the onset temperature of the crystallization was increased to 400°C, suggesting that the MgO seed layer effect on the crystallization of CoFeB was reduced. Note that from Fig. 1(d), the stacks of [MgO 1.2 nm/CoFeB 4 nm]₇ produced (110) and (200) peaks after annealing. These results suggest that the part of the reason why MR reduces with decreasing MgO thickness is related to the mixed orientations in CoFeB due to the poor texture in the thinner MgO barrier. It is important to point out that from the XRD and TEM results, the structure of the crystallized CoFeB turned out to be BCC with lattice constant $a = 0.286$ nm. Therefore, the epitaxial relationship between MgO and CoFeB is similar to the relationship between MgO and Fe [3].

Fig. 2 presents the XRD patterns of Sample B and C. All the samples in Fig. 2 were annealed at 380°C for 30 min. As seen in Fig. 2(a), when the layers adjacent to CoFeB were Ru, a peak appeared at 45.5° after annealing, which is the CoFeB (110) reflection. This was confirmed by HRTEM. Similarly, when NiFe was adjacent to the amorphous CoFeB layer, (110) orientation (peak

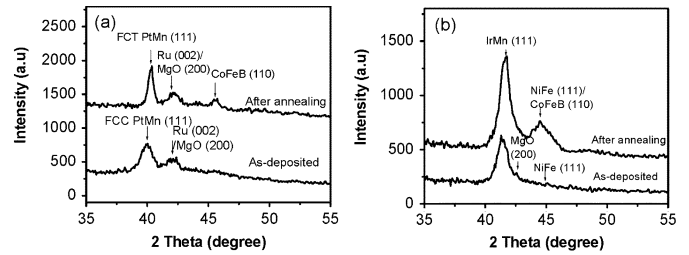


Fig. 2. XRD patterns of (a) Si sub/Ta 10/PtMn 30/CoFe 3/Ru 0.8/CoFeB 3/MgO 2/CoFeB 5/Ru 5, and (b) Si sub/Ta 20 nm/CoFeB 5/MgO 2/CoFeB 5/NiFe 3/ItMn 25/Ta 5 films in nm prior to and post annealing at 380°C.

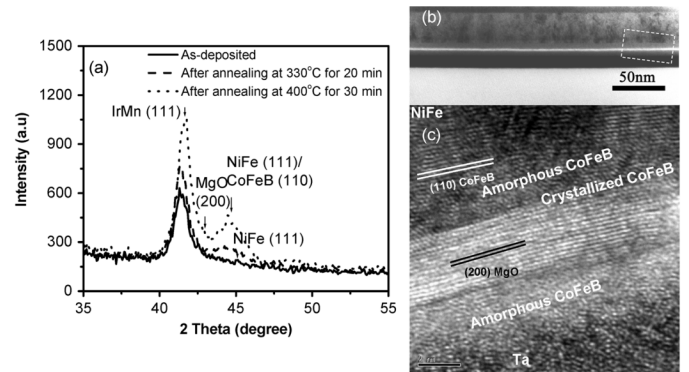


Fig. 3. (a) XRD patterns of the stack of Ta 20 nm/CoFeB 5 nm/MgO 2 nm/CoFeB 5 nm/NiFe 3 nm/IrMn 25 nm/Ta 5 nm as a function of annealing temperature (as-deposited, annealed at 330°C for 20 min, annealed at 400°C for 30 min.) (b) Cross-sectional TEM and (c) HRTEM images of the stacks annealed at 330°C for 20 min. The inset box in (b) indicates the position at which the high resolution image is taken.

at 44.3°) was induced in the CoFeB layer after annealing, as seen in Fig. 2(b). Based on the phase diagram [8], bcc is a stable crystal at room temperature for the bulk alloy of Co₇₅Fe₂₅. In the case of thin films, the interface effect is significant; thus the onset of crystallization, its specific orientation and its crystal structure are closely associated with interfacial energies consisting of chemical (bonding) and structural (lattice distortion) components [6]. We believe the reason that amorphous CoFeB (Co₇₅Fe₂₅) crystallizes in a bcc structure with mostly (110) orientation is due to the close structural match with the strongly (111) textured NiFe and (001) textured Ru. Note that in our case, the structure of the crystallized CoFeB was mostly bcc, which is different from other's report [7].

Fig. 3 shows the XRD patterns and HRTEM images of the stack of Sample C. Initially, our purpose in having this top pinned structure was to obtain a smooth interface between MgO and CoFeB by using an atomically smooth surface of oxidized Si sub/Ta 20 nm/CoFeB 5 nm. This was expected to produce both better crystallinity of the MgO barrier as well as better transport properties in the MTJs. As seen in Fig. 3(b), an almost perfect interface was obtained between MgO and CoFeB. However, after annealing at 330°C for 20 min, CoFeB (110) peak appeared clearly. This suggests that the NiFe layer, which has a strong (111) texture, induces the (110) orientation in the CoFeB layer with much lower onset temperature of crystallization for CoFeB. This is confirmed by the HRTEM image in Fig. 3(b). After annealing at 330°C for 20 min, the crystallization from the MgO/CoFeB interface had only started,

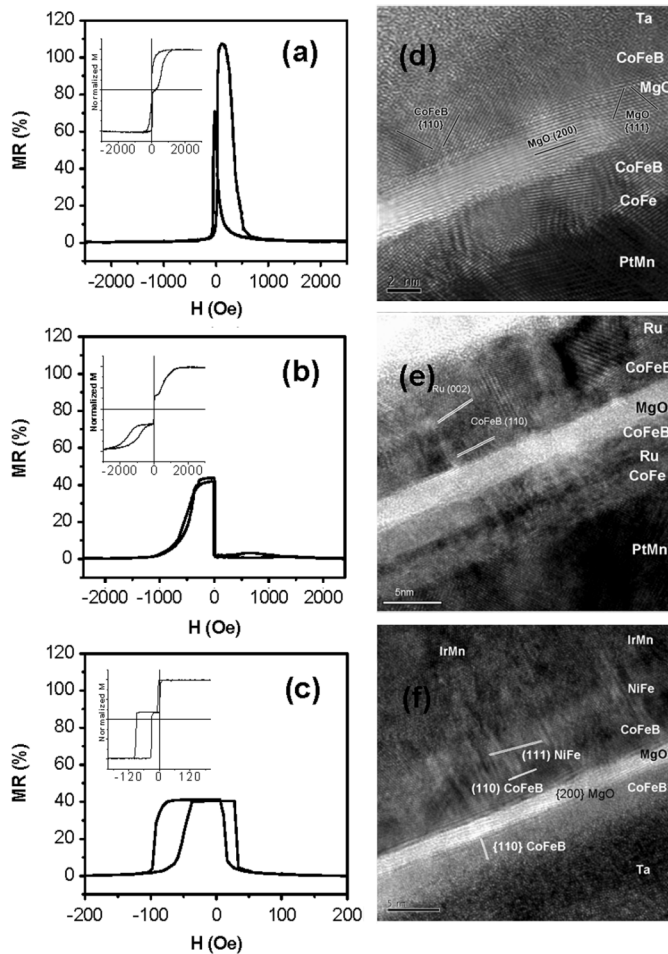


Fig. 4. (a)–(c) Magnetoresistance transfer curves and (d)–(f) HRTEM images of the junction structures of: (a), (d) Ta 10/PtMn 30/CoFe 1.5/CoFeB 2.5/MgO 2 nm/CoFeB 5/Ta 5 nm, (b), (e) Ta 10/PtMn 30/CoFe 3/Ru 0.8/CoFeB 3/MgO 2/CoFeB 5/Ru 5, and (c), (f) Ta 20 nm/CoFeB 5/MgO 2/CoFeB 5/NiFe 3/IrMn 25/Ta 5 nm film stacks annealed at 360°C for 40 min. Insets shown in the left corner in Fig 4. (a)–(c) are MH loops.

while the crystallization from the CoFeB/NiFe interface had already advanced significantly. As the annealing temperature increased, the intensity of both the IrMn (111) peak as well as the CoFeB (110) peak increased, indicating the growth of the grains. These results reveal that the crystallization behavior of the CoFeB layer can be controlled by the adjacent layer. It is worth mentioning that the crystallization of amorphous CoFeB is also related to boron diffusion. The onset temperature for crystallization of amorphous CoFeB can be increased by blocking the diffusion of boron [9].

Fig. 4 shows the M-H loops, transport properties and HRTEM images of the MTJs of Sample A, Sample B and Sample C. The M-H loops shows that Sample A has poor magnetic properties in terms of squareness and exchange bias, while Samples B and C have good magnetic properties. However, Sample A showed highest MR ($\sim 107\%$). The reason for low MR ($\sim 42\%$) for Samples B and C, we believe, is related to the orientation of

the crystallized phase in the CoFeB layers. For the MgO barrier to act as a high efficiency filter, the orientation relationship between MgO and CoFeB should be MgO (100)//bcc CoFeB (100) [3]–[5]. In Sample A, MgO (100)//bcc CoFeB (100) in the MgO/CoFeB interface was observed in Fig. 4(d). In contrast, as seen in Fig. 4(e) and (f), (110) planes were observed in the top CoFeB/MgO interfaces of Samples B and C, respectively. Ru and NiFe, which have hcp (001) and fcc (111) texture, respectively induced (110) planes in CoFeB layer, resulting in poor MR. These results indicate that the magnetic properties as well as the orientation relationship between MgO and CoFeB should be controlled to obtain high MR.

IV. CONCLUSION

The crystallization behavior of the amorphous CoFeB layer in CoFeB/MgO/CoFeB MTJs is critically dependent on the adjacent layers such as Ta, MgO, Ru, and NiFe. When the amorphous CoFeB layer was adjacent to amorphous Ta, (001) textured hcp Ru and (111) textured fcc NiFe, the crystallized CoFeB was bcc with the (110) texture after annealing. The (110) bcc textured CoFeB layers in MTJs result in poor transport properties. These results suggest that the selection of the adjacent to CoFeB is of great significance in the engineering of MgO based MTJ device.

ACKNOWLEDGMENT

This work was supported by STMicroelectronics and the Office of Naval Research.

REFERENCES

- [1] S. S. P. Parkin, C. Kaiser, A. Panchula, P. M. Rice, B. Hughes, M. Samant, and S.-H. Yang, "Giant tunneling magnetoresistance at room temperature with MgO (100) tunnel barriers," *Nature Mater.*, vol. 3, pp. 862–867, 2004.
- [2] S. Yuasa, T. Nagahama, A. Fukushima, Y. Suzuki, and K. Ando, "Giant room-temperature magnetoresistance in single-crystal Fe/MgO/Fe magnetic tunnel junctions," *Nature Mater.*, vol. 3, pp. 868–871, 2004.
- [3] H. W. H. Butler, X.-G. Zhang, T. C. Schulthess, and J. M. MacLaren, "Spin-dependent tunneling conductance of Fe/MgO/Fe sandwiches," *Phys. Rev. B*, vol. 63, pp. 054–416, 2001.
- [4] X.-G. Zhang and W. H. Butler, "Large magnetoresistance in bcc Co/MgO/Co and FeCo/MgO/FeCo tunnel junctions," *Phys. Rev. B*, vol. 70, p. 172 407, 2004.
- [5] C. Park, J. Zhu, M. T. Moneck, Y. Peng, and D. E. Laughlin, "Annealing effects on structural and transport properties of RF-sputtered CoFeB/MgO/CoFeB magnetic tunnel junctions," *J. Appl. Phys.*, vol. 99, pp. 08A901/1–3, 2006.
- [6] D. A. Porter and K. E. Easterling, *Phase Transformations in Metals and Alloys*, 2nd ed. London, U.K.: Chapman & Hall, 1992, ch. 3 & 5.
- [7] S. Yuasa, Y. Suzuki, T. Katayama, and K. Ando, "Characterization of growth and crystallization processes in CoFeB/MgO/CoFeB magnetic tunnel junction structure by reflective high-energy electron diffraction," *Appl. Phys. Lett.*, vol. 87, p. 242 503, 2005.
- [8] T. B. Massalski, *Binary Alloy Phase Diagrams*. Materials Park, OH: ASM International, 1990, vol. 2, pp. 1186–1187.
- [9] Y. Wang, W. Chen, S. Yang, K. Shen, C. Park, M. Kao, and M. Tsai, "Interfacial and annealing effects on magnetic properties of CoFeB thin films," *J. Appl. Phys.*, vol. 99, pp. 08M307/1–3, 2006.